RSC Advances

PAPER

View Article Online
View Journal | View Issue

Cite this: *RSC Adv.*, 2026, **16**, 12915

Dibenzo-18-crown-6/poly-2-aminobenzenethiol based potentiometric sensor for diltiazem determination: greenness assessment

Ghada Ahmed El Sayed,[a] Sahar Mahmoud Mostafa,[a] Mohamed Rabia,[b] Mohamed Ali Korany[a] and Mohamed Magdy Khalil *[a]

A green, cost-efficient, highly selective, and sensitive carbon paste potentiometric sensor for Diltiazem hydrochloride (DTZ) was developed, described, and employed for drug monitoring. With a detection limit of 4.6 $\times$ 10^{-7} mol L^{-1}, the developed sensor exhibits a Nernstian slope of 57.4 $\pm$ 0.81 mV $decade^{-1}$ over a linear concentration range of 1.0 $\times$ 10^{-6} to 1.0 $\times$ 10^{-2} mol L^{-1}. The prepared sensor was stable over a pH range of 2.0–8.0 and responded rapidly (in less than 10 seconds). Additionally, the sensor showed a 6 weeks lifespan. A conducting polymer of poly-2-aminobenzenethiol was characterized using X-ray diffraction (XRD) and scanning electron microscopy (SEM). The surface properties of the proposed sensor were characterized by electrochemical impedance spectroscopy (EIS). The sensor was successfully applied for the determination of DTZ with acceptable recovery values in pure formulations, pharmaceutical formulations, human urine, and industrial water samples. The effectiveness of the suggested sensor in industrial water and a complicated urine matrix leads to its potential use in hospitals for quick diagnosis of overdose patients and for pharmaceutical industry quality control and assurance. In addition to experimental evaluation, the sensor's greenness, practicality, and analytical performance were comprehensively assessed using the Analytical GREEnness metric (AGREE), the Analytical Eco-scale, the Blue Applicability Grade Index (BAGI), and the Red Analytical Performance Index (RAPI).

Received 10th October 2025
Accepted 9th February 2026

DOI: 10.1039/d5ra07743e

rsc.li/rsc-advances

1. Introduction

Globally, cardiovascular diseases (CVDs) are the leading cause of death, accounting for 17.9 million deaths per year.[1,2] Hypertension is referred to as a "silent killer". The World Health Organization (WHO) reports that it is the most significant risk factor for the occurrence of various cardiovascular conditions, including myocardial infarctions, strokes, renal failure, and eventually death.[3] Nowadays, over 1 billion people around the world suffer from hypertension, and by 2025, 1.5 billion people are expected to be affected by hypertension worldwide.[4] Among the various classes of antihypertensive drugs, Diltiazem hydrochloride (DTZ) stands out as a calcium channel blocker (CCB) that helps dilate blood vessels (angiectasis) by inhibiting

[a]*Chemistry Department, Faculty of Science, Beni-Suef University, Beni-Suef, Egypt. E-mail: magdy_mmagdy@yahoo.com; mohamed.mahmoud@science.bsu.edu.eg; mohamedali_k@outlook.com*

[b]*Nanomaterials Science Research Laboratory, Chemistry Department, Faculty of Science, Beni-Suef University, Beni-Suef, 62514, Egypt*

Ghada Ahmed El Sayed

Ghada Ahmed Elsayed holds a Bachelor's degree in Chemistry and a master's degree in Analytical Chemistry, both from Beni-Suef University, Egypt. Her research focuses on the development of electroanalytical sensors for detecting and monitoring analytes in liquid samples, with a focus on improving sensor sensitivity, selectivity and reliability.

Sahar Mahmoud Mostafa

Sahar Mahmoud Mostafa received her PhD degree in Analytical Chemistry from the Faculty of Science, Beni-Suef University, Egypt in 2021. She is a lecturer of analytical chemistry at the Department of Chemistry, Faculty of Science, Beni-Suef University, Egypt. Her research work is focused on ion-selective electrodes.

calcium influx into vascular smooth muscle cells, helping in hypertension, cardiac arrhythmias, and angina.[5] Cardiovascular drugs are known to be potentially lethal in overdosage and according to a previous study, an overdose of DTZ may cause chest pain, slow heartbeat, fainting, and hypotension and may lead to death.[6] Consequently, there is an urgent need for a simple, rapid, sensitive, and accurate method for detecting DTZ in biological fluids, pharmaceutical formulations and bulk. A careful review of the literature showed that a variety of techniques for detecting DTZ have been reported, including high-performance thin-layer chromatography (HPTLC),[7] micellar per aqueous liquid chromatography (MPALC),[8] gas chromatography,[9] spectrophotometry,[10] Adsorptive Stripping Voltammetry[11,12] and potentiometry.[13] Chromatography is one of the instrumental procedures that offer the highest level of selectivity and sensitivity. These techniques, however, have significant disadvantages that make them undesirable, including reliance on costly and sophisticated equipment, the necessity of skilled operators to carry out the preconcentration and sample preparation procedures, prolonged analysis time, and the high consumption of hazardous organic solvents. UV-visible spectrophotometry is a straightforward analytical technique, but the primary drawbacks are the lack of selectivity, low sensitivity and requirement for the derivatization. To overcome these problems, several chemometric tools and a preconcentration process have been added, which significantly extends the analysis time.[14,15] The consumption of the analyte is a fundamental aspect of voltammetric techniques. Small volumes might cause struggling to monitor low concentrations, and catalyzed oxidation may cause additional challenges since the analyte moves slowly from the sample bulk to the sensor surface.[16] Potentiometry using ion-selective electrodes (ISEs) is distinguished from automated techniques by the use of safe solvents that are environmentally friendly, the absence of sample pretreatment or destruction, low energy consumption, cost-effectiveness, rapidity, flexibility of onsite application, portability, and ease of handling. In spite of having a renewable surface and being readily adjustable, carbon paste sensors (CPSs) meet all of the aforementioned requirements, producing electrochemical sensors that are robust, sensitive, and repeatable.[17–19] Herein, a neutral Lipophilic ionophore Dibenzo-18-crown-6 (DB18C6) – based Carbon paste sensor was synthesized, characterized and tested for the determination of DTZ in pure formulations, pharmaceutical formulations, human urine, and industrial water samples. Significant improvements have been achieved in electrochemistry as a result of the development of nanomaterials and polymers. Their outstanding features, including enlarged active surface area, electrocatalytic activity, and high electrical conductivities, have led to their broad application in the production of electrochemical sensors/biosensors, supercapacitors, and fuel cells,[20] these nanomaterials are divided into various categories depending on their morphology, size and physical and chemical properties.[21] Conducting polymers represent a promising class of materials for electrochemical applications due to their large surface area and cost-effective mass production techniques. Among these, polythiophene derivatives stand out because they offer not only significant surface area but also high electrical conductivity and favorable morphological properties. These attributes make polythiophene derivatives particularly suitable for a variety of electrochemical tests, enhancing their performance in applications such as sensors, batteries, and supercapacitors. The combination of cost-efficiency in production and superior

Mohamed Rabia

Mohamed Rabia received his PhD and MSc degrees from Beni-Suef University in 2015. He is currently an assistant professor at the Department of Chemistry, Faculty of Science, Beni-Suef University. His research interests are electrochemical sensors, gas sensors, functional polymer materials, solar cells, and hydrogen generation.

Mohamed Ali Korany

Mohamed Ali Korany received his BSc and MSc degrees in Chemistry from the Faculty of Science, Beni-Suef University, Egypt. He received his PhD from the Department of Chemistry, Faculty of Science, Beni-Suef University, Egypt. His research is focused on ion-selective electrodes.

Mohamed Magdy Khalil

Mohamed Magdy Khalil received his PhD degree in Analytical Chemistry from the Polytechnical Institute, Bucharest, Romania in 1984. He is a professor of Analytical Chemistry at the Department of Chemistry, Faculty of Science, Beni-Suef University, Egypt. His research work is focused on ion-selective electrodes. He is also interested in complexation equilibria and determination of the stability constants of binary and ternary complexes involving biologically active ligands.

electrochemical properties underscores the potential of conducting polymers in advancing electrochemical technologies.[22,23] Nihal *et al.* developed a dopamine molecularly imprinted poly(*O*-phenylenediamine) sensor.[24] A molecularly imprinted electrochemical sensor (MIP/DA) for selective and sensitive determination of dopamine (DA) was fabricated by electrochemical polymerization of *p*-aminothiophenol in the presence of DA on a gold electrode. The sensor was effectively utilized to determine dopamine concentrations in pharmaceutical samples, with an appropriate linear range and low detection limit. The current study aims to determine (DTZ) in pure formulations, pharmaceutical formulations, human urine, and industrial water samples using a novel sensitive and selective carbon paste sensor based on DB18C6 as an ionophore and *Ortho* nitrophenyl octyl ether (*O*-NPOE) as a plasticizer, as well as a poly-2-aminobenzenethiol modifier to improve the potentiometric behavior of the investigated sensors. Fourier transform infrared (FTIR), X-ray diffraction (XRD), and scanning electron microscopy (SEM) were utilized to characterize poly-2-aminobenzenethiol. Greenness evaluation of the proposed method was performed using the Analytical GREEnness metric and Analytical Eco-scale while the sensor's applicability and overall analytical performance were further assessed using the BAGI and RAPI metrics.

2. Experimental

2.1 Reagents and materials

In this study, only analytical-grade compounds were used. Deionized water was used throughout all experiments. Pure Diltiazem hydrochloride (DTZ) was supplied by EIPICO, Egypt. The pharmaceutical formulation (ALTIAZEM®) was purchased from local drug stores. Verapamil hydrochloride was given by Abbott, Cairo, Egypt. Spectroscopic graphite powder (1–2 mm) was purchased from Sigma-Aldrich, sodium tetraphenylborate (NaTPB) was obtained from Fluka (U.S.A.). The sensor plasticizers were as follows: Ortho nitrophenyl octyl ether (*O*-NPOE, sigma) and dibutyl phthalate (DBP, Merck). Dibenzo-18-crown-6 (DB18C6) was purchased from Euromedex, France. The metal salts were provided by BDH (UK) as nitrates or chlorides. 2-Aminobenzenethiol (99.9%) was acquired from VWR company, Germany. Standard solution of 1.0×10^{-2} mol L^{-1} DTZ was freshly prepared by dissolving the accurately weighed amount in deionized water. Working solutions (1.0×10^{-7}–1.0×10^{-2} mol L^{-1}) of the drug were prepared. Concentrated solutions of NaOH and HCl were used within the range (0.1–1.0 mol L^{-1}) for adjusting pH of the medium.

2.2 Equipment

Metrohm 702 SM Titrino (Metrohm, Switzerland) was employed for potentiometric and pH measurements to ensure accurate analysis. The crystallinity and primary crystal phases were determined based on XRD patterns using a PANalytical-Empyrean X-ray diffractometer, operating within a detection range of 20° to 40°. To analyze the chemical composition of poly-2-aminobenzenethiol, a Fourier transform infrared spectrometer (FTIR8400S; Shimadzu) was utilized within a frequency range of 750.0 cm^{-1} to 3500.0 cm^{-1}. Furthermore, scanning electron microscopy (SEM) images were obtained using a ZEISS SUPRA 55 VP and ZEISS LEO (Gemini Column) for detailed morphological characterization.

2.3 Preparation of the poly-2-aminobenzenethiol

The synthesis of poly-2-aminobenzenethiol is carried out through the oxidative polymerization of 2-aminobenzenethiol using $(NH_4)_2S_2O_8$ as the oxidizing agent in an acidic medium. The reaction takes place in the presence of 1.2 mol L^{-1} HCl, which facilitates the polymerization process. The molar ratio of monomer to oxidant is carefully controlled at 1 : 2.5, ensuring an optimal reaction environment for polymer formation, with the initial monomer concentration set at 0.06 mol L^{-1}.

The polymerization process is initiated by the gradual addition of the oxidant to the monomer solution under continuous stirring. As the reaction progresses, the formation of a dark precipitate is observed, which serves as a visual indication of successful polymer synthesis. This precipitate consists of poly-2-aminobenzenethiol, confirming that the polymerization has proceeded effectively.

Upon completion, the precipitated polymer was collected by vacuum filtration and subjected to a rigorous multistep purification protocol. The material was first washed repeatedly with large volumes of deionized water until the filtrate reached neutral pH, confirming the effective removal of residual hydrochloric acid and persulfate-derived ionic species. This step is critical to eliminate mobile ions that could artificially contribute to electrical conductivity. The polymer was then washed several times with absolute ethanol to remove unreacted monomer, oligomeric fragments, and weakly adsorbed organic impurities. A final rinse with an ethanol–water mixture (1 : 1, v/v) was performed to ensure comprehensive purification.

The purified poly(2-aminobenzenethiol) was dried at a moderate temperature until a constant mass was obtained. These purification and drying steps ensure that the measured conductivity arises exclusively from the intrinsic conjugated polymer backbone, rather than from residual ionic oxidants or acidic residues.

2.4 Sensors construction

Different ratios of Dibenzo-18-crown-6 (DB18C6) ionophore, poly-2-aminobenzenethiol, NaTPB (a lipophilic anionic additive), spectroscopic graphite powder and plasticizers were blended in a Petri dish to form a homogeneous moist paste, which was then inserted into the tip of a polypropylene sensor body.[25] The paste was polished to a glossy finish using smooth paper. Potentiometric measurements were performed on the constructed sensor after soaking for 30.0 minutes in a solution containing 1.0×10^{-3} mol L^{-1} DTZ.

2.5 Standard solutions and sample preparation

Simple series of dilutions using deionized water were used to prepare concentrations ranging from 1.0×10^{-2} mol L^{-1} to 1.0×10^{-7} mol L^{-1} from a stock solution of DTZ (1.0 ×

10^{-2} mol L^{-1}). For analytical application, ten ALTIAZEM® tablets were weighed, ground, dissolved in distilled water, filtered, and the filtrate was diluted to 250 mL to prepare 1.0×10^{-4} mol L^{-1} DTZ, which was used for preparing a series of diluted solutions using deionized water.

2.6 Analytical applications

Transferring 3, 6, and 9 mL of 1.0×10^{-2} mol L^{-1} DTZ solution to a 50 mL beaker, the sensor was used as an indicator and titrated with a standard solution of 1.0×10^{-2} mol L^{-1} Na-TPB. The end points were determined from the S-shaped curve. The standard addition method was applied by adding small increments of 1.0×10^{-2} mol L^{-1} of DTZ solution to 50 mL aliquot samples of various concentrations of pure drug, pharmaceutical formulation, human urine, and industrial water.

3. Results and discussion

Potentiometric ion selective electrodes (ISEs) are the best option for routine analysis since they eliminate the need for sample pretreatment immediately, which is a major challenge in monitoring DTZ in pure drugs and pharmaceutical formulations. This avoids interference from contaminants during analysis.

3.1 Crystal structure and morphology

The chemical analysis of the synthesized poly-2-aminobenzenethiol is illustrated in Fig. 1(a). FTIR spectroscopy provides detailed information on the polymer's functional groups. The primary functional groups are identified by their characteristic vibration bonds under the IR spectrum. The benzene ring-related groups, including C–C, C=C and N–C, are observed at 1619, 1514, 1310, 1221, and 1126 cm^{-1}.[26,27] Additionally, other functional groups are detected at 1039, 875, and 755 cm^{-1}, corresponding to the para positions under the disubstituted groups. A peak at 3366 cm^{-1} is associated with the N–H and S–H groups, characteristic of this thiophene polymer.

The XRD pattern of the pristine poly(2-aminobenzenethiol), presented in Fig. 1b, exhibits distinct diffraction features that indicate the presence of short-range ordered domains within the polymer matrix. A set of well-defined reflections appearing in the 2θ range of 24.5°–29.5° suggests the development of a semi-crystalline, promising polymer, arising from partial chain alignment and intermolecular interactions among the conjugated polymer backbones. This semi-crystalline character is consistent with conducting polymers prepared *via* oxidative polymerization and supports efficient charge transport while preserving the structural flexibility required for sensing applications.[28]

Moreover, the morphological and topographical properties of the synthesized polymer are examined through SEM images, shown in Fig. 1(c) and (d) at various magnifications. The polymer forms porous spherical particles with an average size of 260 nm. Each spherical particle exhibits its own porosity, significantly increasing the surface area. This enhanced surface area is particularly advantageous for applications in sensing technologies, where a large surface area can improve sensitivity and performance.[29]

3.2 Optimization of the sensor matrix

The sensor composition was improved by adjusting the amount of ionophore (DB18C6), ionic additive (Na-TPB), plasticizer type

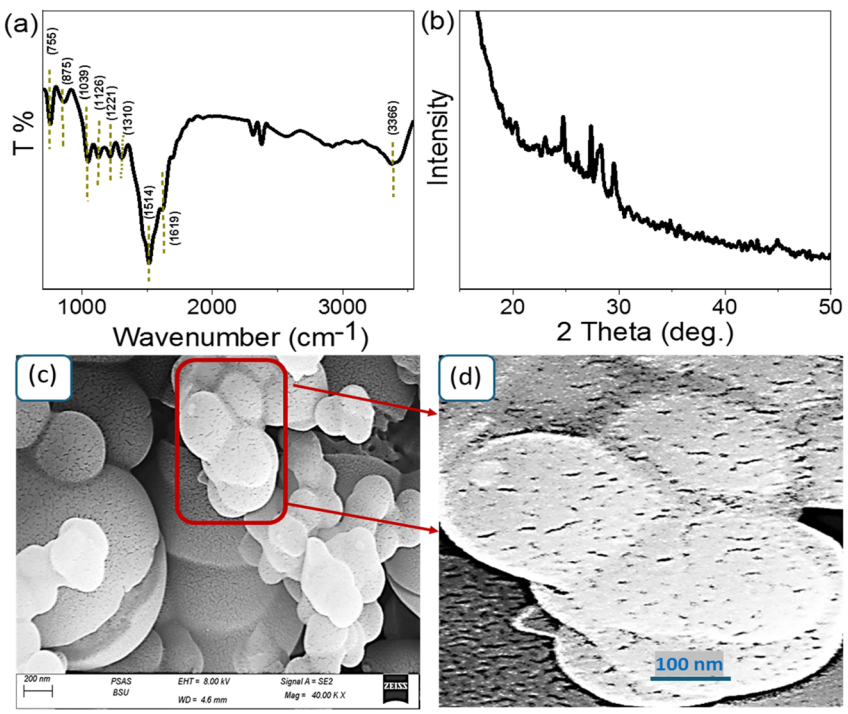

Fig. 1 The chemical analyses of the synthesized poly-2-aminobenzenethiol: (a) FTIR, (b) XRD and (c and d) SEM images of the synthesized poly-2-aminobenzenethiol.

(DBP and *O*-NPOE), and modifier (poly-2-aminobenzenethiol). Different types of ionophores natural as (Chitosan) and synthetic as (18-crown-6 and Dibenzo-18-crown-6) were tested, results showed that sensors based Dibenzo-18-crown-6 (DB18C6) ionophore exhibited best potentiometric response compared with those based on the other ionophores. This can be attributed to the ability of crown ethers to bind ions selectively and to form stable inclusion complex between ionophores and the target drug cation.[30] Several sensors were fabricated with different DB18C6 percentages ranging from 0.30% to 1.0% (w/w relative to carbon powder), to exhibit a Sub- Nernstian response towards DTZ of 33.0 mV decade^{-1} with 0.70% DB18C6. The utilization of neutral ionophores requires the presence of appropriate ion-exchange sites, which can create more robust, partially covalent, or host-specific interactions between these species and ions.[31] For that reason, NaTPB anionic site was integrated into the paste with a percentage of 0.70% to result in a super-Nernstian slope of 77.0 mV decade^{-1}. The amount of NaTPB was optimized to 0.50%, yielding improved sensor performance, including a Nernstian slope of (50.0 mV decade^{-1}), a linear range of (1.0×10^{-5}–1.0×10^{-2} mol L^{-1}), and a low detection limit of (8.30×10^{-6} mol L^{-1}). This significant improvement in sensor response is ascribed to the incorporation of the NaTPB anionic additive, which enhances primary ion selectivity, increases paste conductivity, decreases or eliminates co-ion interference, and shortens sensor reaction time.[32] Since conducting polymers provide unique advantages, their incorporation into an inert polymeric matrix to produce modified carbon-paste sensors has become a significant advancement in analytical electrochemistry. Poly-2-aminobenzenethiol, a conducting polymer, was added to the paste's matrix to modify the constructed sensor. The data showed that the addition of conducting polymer of poly-2-aminobenzenethiol improved the behavior of the sensor. Therefore, different percentages of poly-2-aminobenzenethiol ranging from 3.0% to 10.0% (w/w relative to carbon powder) were added to the paste matrix to have an optimum composition of 5.0% poly-2-aminobenzenethiol, 0.70% DB18C6, 0.50% NaTPB, 49.40% DBP plasticizer and 44.40% graphite powder. The reasonable enhancement in the sensor's performance is attributed to improving the sensor conductivity and increasing the transduction of the chemical signal to an electrical signal.

The performance of the sensor is improved by the plasticizer's assistance in controlling various equilibria between the major ions and the ionophore in the paste. Khalil *et al.*[33] A previous study investigated a range of natural (apricot, almond, and castor oil) and synthetic (DBP, DOS, DOA, and DOP) plasticizers and concluded that DBP was the most effective. Introducing a new member to the plasticizer family is crucial for future feature enhancements of the sensor. Two carbon paste sensors were created using *O*-NPOE ($\varepsilon = 24$) as a solvent mediator and DBP ($\varepsilon = 6.4$). When compared to the sensor plasticized by DBP, the sensor plasticized by *O*-NPOE exhibits a better potentiometric response with a Nernstian slope of (57.4 ± 0.81 mV decade^{-1}), a linear range of (1.0×10^{-6}–1.0×10^{-2} mol L^{-1}), a low detection limit of (4.6×10^{-7} mol L^{-1}), and excellent potential reading stability (Fig. 2). *O*-NPOE suitability

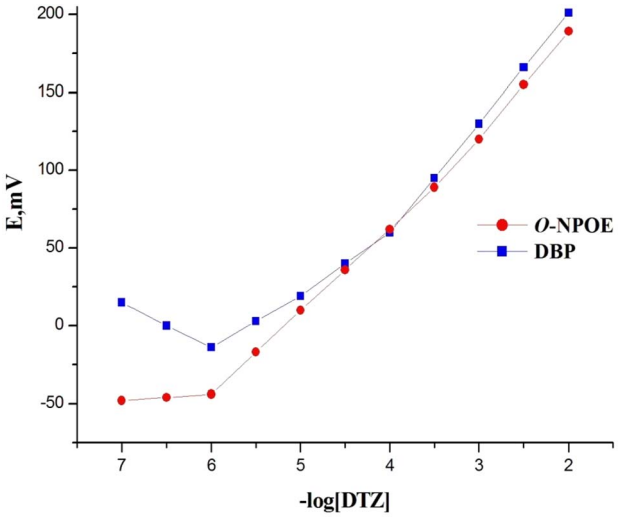

Fig. 2 Calibration curves of DTZ-CP sensor at optimum paste composition plasticized with DPB and *O*-NPOE.

can be attributed to its high lipophilicity and dielectric constant, which allows *O*-NPOE to readily incorporate ionophores into the sensor's matrix, ensuring effective ion transport and sensing.[34] The limit of quantification (LOQ), calculated as $10\sigma/S$, was found to be 1.52×10^{-6} M. Although this value is slightly higher than the minimum calibration point, it represents the lowest concentration that can be reliably quantified with acceptable accuracy and precision. While measurable signals can be observed below the LOQ, only concentrations at or above this level satisfy the statistical criteria for accurate and precise quantitative analysis.[35] Based on these considerations *O*-NPOE was selected for all subsequent tests (Table 1).

3.3 Electrochemical impedance spectroscopy (EIS)

The electrochemical impedance analysis of the fabricated sensor, as illustrated in Fig. 3, reveals significant improvements in both *c* (R_S) and charge transfer resistance (R_{CT}) when compared to the blank sample. The sensor demonstrates a well-defined semicircle in the Nyquist plot, with R_S and R_{CT} values of 84 Ω and 560 Ω, respectively, whereas the blank sample exhibits higher resistance values of 180 Ω and 1120 Ω (Fig. 3). This considerable reduction in resistance suggests a notable enhancement in electrochemical charge transfer, both within the solution and across the sensor's interface.

The improved charge transfer characteristics indicate a strong interaction between the sensor and the electrolyte solution, likely facilitated by efficient charge attraction mechanisms. The superior sensitivity of the sensor can be attributed to the formation of van der Waals interactions, which enhance the interface conductivity and improve charge transport efficiency. The lower resistances observed further highlight the sensor's enhanced electrochemical performance, confirming its ability to facilitate rapid and effective electron transfer. These findings align well with recent scientific studies,[36] reinforcing the sensor's potential for high-sensitivity electrochemical applications. This enhancement underscores the importance of the

Table 1 Performance characteristics of DTZ-CP sensor[a]

Parameter	DTZ-CP
Composition	0.70% DB18C6 + 0.50% NaTPB + 5.0% poly-2-aminobenzenethiol + 44.40% graphite + 49.40% *O*-NPOE
Slope (mV decade^{-1})	57.4 ± 0.81
Correlation coefficient (r^2)	0.997
RSD (%)	1.41
LOD (mol L^{-1})	4.6×10^{-7}
LOQ (mol L^{-1})	1.52×10^{-6}
LR (mol L^{-1})	1.0×10^{-6}–1.0×10^{-2}
Response time (s)	≤10
Working pH range	2.0–8.0
Isothermal coefficient (mV °C^{-1})	0.00023
Life time (weeks)	6.0

[a] LOD: limit of detection, LOQ: limit of Quantification, LR: Linear range, RSD: relative standard deviation (three determinations).

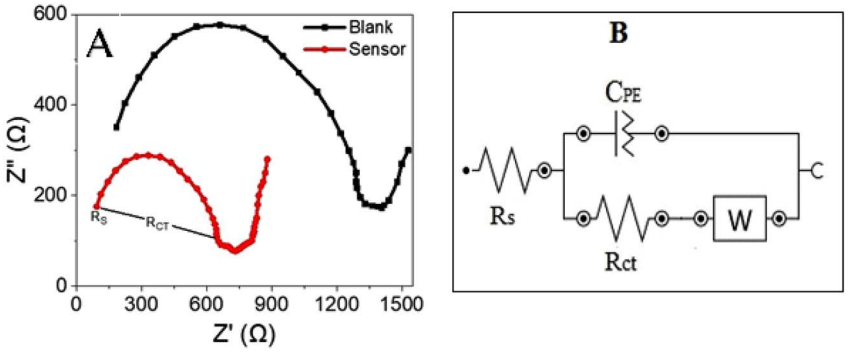

Fig. 3 EIS of DTZ-CP sensor against the blank sensor (A), and Equivalent circuit (B).

sensor's structural properties in optimizing its overall efficiency.

3.4 Sensor potential response characteristics

The constructed sensor's fast potential response demonstrates its suitability for focused ion monitoring. The dynamic response time of the developed sensor was investigated by immersing it in a series of working solutions ranging from 1.0×10^{-7} to 1.0×10^{-2} mol L^{-1}, each with a 10-fold difference, and the time required to achieve the steady state potential (within ±1 mV) was monitored.[37] Fig. 4 shows that the examined sensor reached potential equilibrium in around 10 seconds. The reversibility of the sensors was checked by recording the sensor response in the sequence high-to-low from 1.0×10^{-2} to 1.0×10^{-7} mol L^{-1} sample concentrations of DTZ. The results showed that the response of the sensors was reversible and has no memory effect (Fig. 4). The repeatability of potential reading was tested by immersing the constructed sensor in successive high-to-low concentrations (1.0×10^{-3} and 1.0×10^{-4} mol L^{-1}). The relative standard deviation (RSD) of five replicate measurements was 1.34% for 1.0×10^{-4} mol L^{-1} and 0.89% for 1.0×10^{-3} mol L^{-1} confirming the high precision of the sensor and the consistency of the sensor's output over consecutive measurements. On the other hand, to evaluate reproducibility, five independent sensors were constructed and checked in 1.0×10^{-5} mol L^{-1} DTZ solution, the RSD values of their potentiometric responses found to be 1.87%, indicating the reliability, accuracy, and quality of a sensor's measurements.

3.5 Water layer test

An essential step in verifying solid-contact ion-selective sensors is the water layer test. Potential drifts, common in solid-contact electrodes, are more evident when a water layer is present.[38] To perform the water layer test, the sensor potential was recorded sequentially after conditioning in 1.0×10^{-3} mol L^{-1} DTZ solution, followed by immersion in 1.0×10^{-3} mol L^{-1} verapamil hydrochloride interferent solution, and finally returning to 1.0×10^{-3} mol L^{-1} DTZ solution. No water layer was observed, as indicated by the absence of potential drift (Fig. 5). This behavior is attributed to the high hydrophobicity of the developed carbon paste sensor.

3.6 Effect of pH

The working pH range is a controlling factor that restricts the use of an ion selective electrode. The behavior of the sensor response with pH change was studied for DTZ solutions (1.0×10^{-4} and 1.0×10^{-3} mol L^{-1}) covering a wide pH range (1.5–12.0). The constructed sensor is stable during a broad pH range of 2.0–8.0, as shown in Fig. 6. This broad pH range demonstrates the sensor's applicability across various types of media matrices. At lower pH values, the mV measurements dropped owing to the hydronium ion's interference.[39] At pH values above

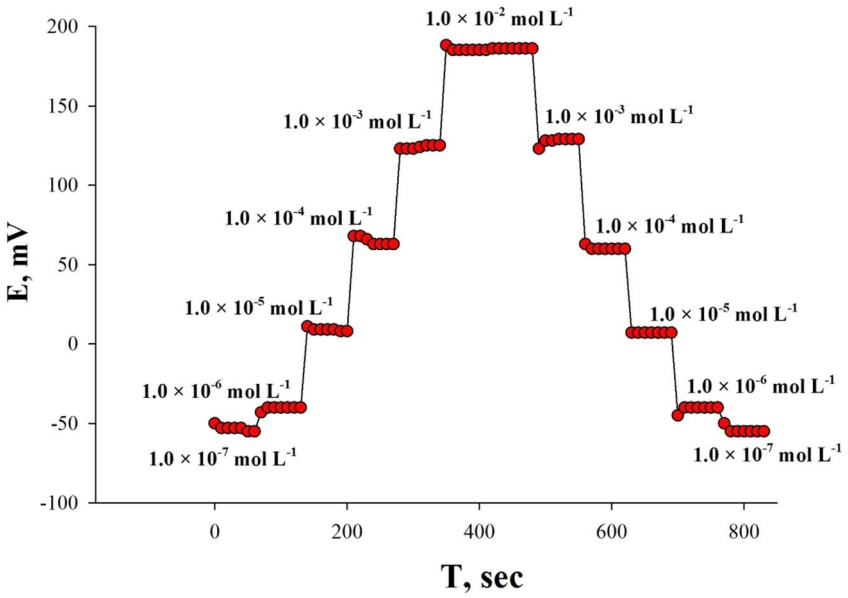

Fig. 4 Dynamic response time and reversibility of DTZ-CP sensor.

8, a noticeable drop in potential is observed. This behavior is primarily attributed to the proximity of the solution pH to the pK_a of diltiazem (~7.7). Near this pH, a deprotonating of the amine group occurs. Consequently, the concentration of the protonated diltiazem species responsible for the potentiometric response decreases, leading to a reduction in the measured potential.

3.7 Selectivity

An essential characteristic for assessing a sensor's ability to discriminate between the analyte ion and other interfering species in the same solution is selectivity behavior.

Quantitative evaluation of the selectivity behavior was carried out by calculating the logarithmic potentiometric selectivity coefficients ($\log K^{pot}_{DTZ, J^{z+}}$). The separate solution method (SSM)[40] was employed for inorganic cations (K^+, Na^+, Li^+, NH_4^+, Mg^{2+}, Ca^{2+}, and Verapamil), whereas the matched potential method (MPM)[41,42] was used for biologically relevant species commonly found in urine, including amino acids (glycine, histidine, and DL-alanine) and sugars (glucose and fructose). As shown in Table 2, all investigated interfering species exhibited negligible interference, except for K^+, which showed moderate interference, confirming the sensor's ability to accurately determine diltiazem in real urinary samples.

In addition to SSM and MPM, Bakker protocol was applied.[43] According to this approach, sensor selectivity is governed by the ion-exchange equilibrium established at the membrane/solution interface as well as by the relative mobility of ions within the membrane matrix. The influence of potentially interfering inorganic cations on the potentiometric response

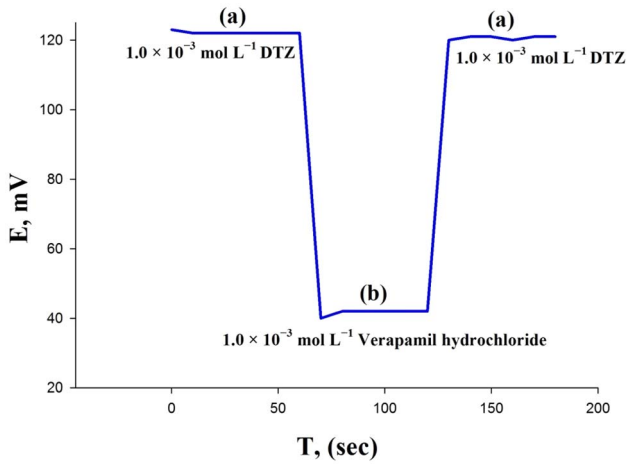

Fig. 5 Water layer test for DTZ-CP sensor in (a) 1.0 × 10^{-3} mol L^{-1} Diltiazem hydrochloride and (b) 1.0 × 10^{-3} mol L^{-1} Verapamil hydrochloride.

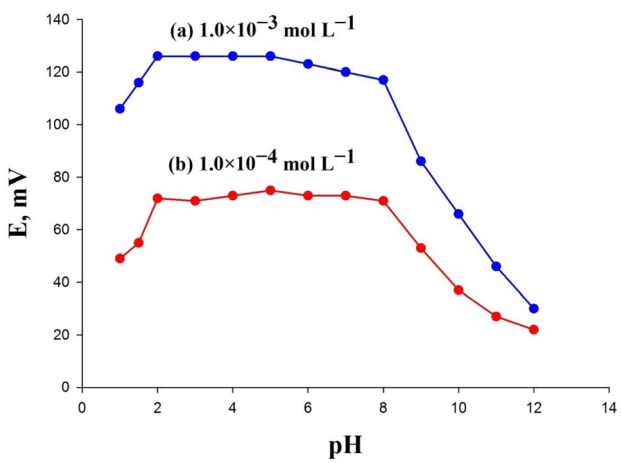

Fig. 6 Impact of pH on the potential response of DTZ-CP sensor for (a) 1.0 × 10^{-4} and (b) 1.0 × 10^{-3} mol L^{-1} DTZ solutions.

Table 2 Logarithmic potentiometric selectivity coefficient of DTZ-CP sensor

$\log K^{pot}_{DTZ,\ J^{Z+}}$		
Interferent	SSM	MPM
K^+	−0.90	—
Na+	−1.90	—
NH_4^+	−1.60	—
Li^+	−2.60	—
Mg^{2+}	−3.83	—
Ca^{2+}	−3.71	—
$Verapamil^+$	−1.38	—
Hestidine	—	−1.04
DL-Alanine	—	−1.13
Glycine	—	−1.50
Glucose	—	−1.30
Fructose	—	−1.20

was examined by recording the electrode potential as a function of −log[concentration] of the added interfering ions. The selectivity of the investigated sensor toward the primary ion was further assessed by constructing calibration plots for several cationic species, namely K^+, Na^+, NH_4^+, Li^+, Mg^{2+}, and Ca^2, in addition to Verapamil as a structurally related drug. As shown in Fig. 7, no significant response was observed for the interfering species tested, except for K^+, which showed a limited response. This behavior can be attributed to the high affinity of dibenzo-18-crown-6 (DB18C6) for K^+relative to other alkali metal cations.[44] Crown ethers are macrocyclic host molecules with a cavity that selectively coordinates cations through the lone pairs of oxygen atoms.[45] The strong binding of DB18C6 to K^+ arises from the close match between the potassium ion radius and the crown ether cavity. This size complementarity enables the formation of unusually stable K^+ complexes, explaining the limited potentiometric response observed.

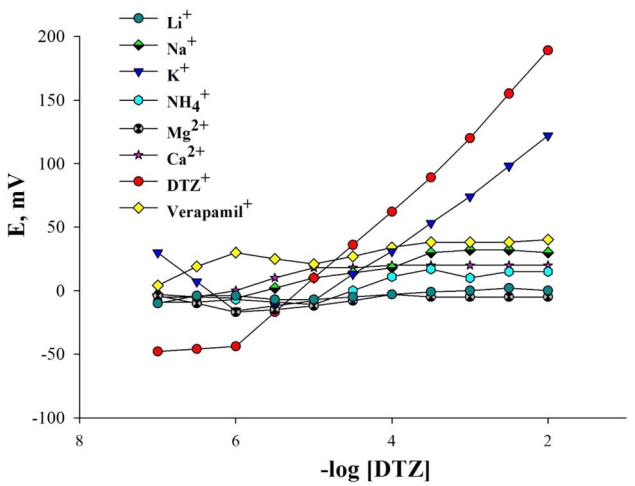

Fig. 7 Response of DTZ-CP sensor to DTZ and some interfering species.

3.8 Life span and thermal stability

The lifetime of the sensor was evaluated by measuring its performance parameters on a daily basis. Over six weeks, the sensor maintained a stable response slope and the same linear dynamic range. After this period, a considerable decrease in response slope was observed, along with a narrower linear dynamic range.

Calibration curves were plotted at various test solution temperatures ranging from 20 °C to 60 °C to investigate thermal stability. Trace changes were noticed in the slope, dynamic range and detection limit of the constructed sensor up to 50 °C with a thermal coefficient value of 0.00023 V $°C^{-1}$. Despite this, exceeding temperatures beyond 50 °C led to a substantial variance from the theoretical values. This suggests high temperatures may cause deterioration of the sensor's outer layer. Furthermore, some leaching from the paste may occur, compromising overall sensor responsiveness.

3.9 Application of synthesized sensor

It is critical to evaluate the applicability of the modified sensor; therefore, the drug was examined in pure drug, pharmaceutical formulations, human urine, and industrial water samples using potentiometric titration and the standard addition method. As shown in Table 3, the sensor accurately measured DTZ concentrations.

In the potentiometric titration, the constructed sensor was effectively employed as an indicator for detecting the endpoint of DTZ (Fig. 8). To evaluate possible matrix effects, the concentration of DTZ was determined by the standard addition method in pure solutions, ALTIAZEM® (60 mg per tablet), biological fluid (urine) and industrial water samples. As shown in Table 3, the sensor achieved recoveries ranging from 97.0% to 102.0%, with RSD values below 1.95%.These results demonstrate negligible matrix effects and confirm the sensor's efficiency in measuring DTZ in pharmaceutical preparations and pure solutions.

3.10 Comparison with reported methods

Compared to other electroanalytical techniques and other methods for determining DTZ in terms of simplicity, sensitivity, and cost-effectiveness. In some ways, our method is more accurate than those reported in the literature, and comparable in others. No sample pretreatment is required, as the sensor is prepared simply using inexpensive reagents, making it superior to previously reported methods. In addition, the constructed sensor exhibited a linear range of (1.0×10^{-6}–1.0×10^{-2} mol L^{-1}) wider than the reported data in Table 4 and a detection limit of (4.6×10^{-7} mol L^{-1}), outperforming spectrophotometric[10] and Potentiometric[13] techniques. The sensor was also used to determine the concentration of DTZ in pure formulations, pharmaceutical formulations, human urine, and industrial water samples, yielding accurate results with a low detection limit.

3.11 Greenness assessment

Global efforts to develop green analytical methods that may help reduce and/or completely eliminate the use and

Table 3 Application of the proposed sensor for determination of DTZ in pure, pharmaceutical, urine and Industrial water preparations and the statistical parameters using standard addition method and potentiometric titration method

Sample	Statistical parameters	Standard addition method			Potentiometric titration method		
		Taken mg	Recovery (%)	RSD (%)	Taken mg	Recovery (%)	RSD (%)
Pure solution		0.23	97.00	1.00	13.53	100.00	1.95
		1.13	97.30	0.89	27.06	97.00	1.69
		2.26	98.60	1.87	40.59	102.20	1.27
	Mean ± SD		97.60 ± 0.85			99.7 ± 2.6	
	N		3			3	
	F- ratio		1.6 (9.28)[a]				
	t-test		1.8 (2.77)[b]				
Altiazim (60 mg per tablet)		0.23	97.00	0.45	13.53	97.00	1.97
		1.13	97.40	0.61	27.06	100.00	0.96
		2.26	101.30	0.56	40.59	97.00	1.72
	Mean ± SD		98.57 ± 2.4			98.00 ± 1.70	
	N		3			3	
	F- ratio		3.27 (9.20)[a]				
	t-test		1.30 (2.77)[b]				
Urine		0.23	97.00	1.06			
		1.13	99.50	1.31			
		2.26	98.30	1.03			
	Mean ± SD		98.27 ± 1.27				
Industrial water		0.23	101.50	1.59			
		1.13	102.00	2.09			
		2.26	97.00	1.10			
	Mean ± SD		100.17 ± 2.7				

[a] Tabulated *F*-value at 95% confidence level. [b] Tabulated *t*-value at 95% confidence level and four degrees of freedom.

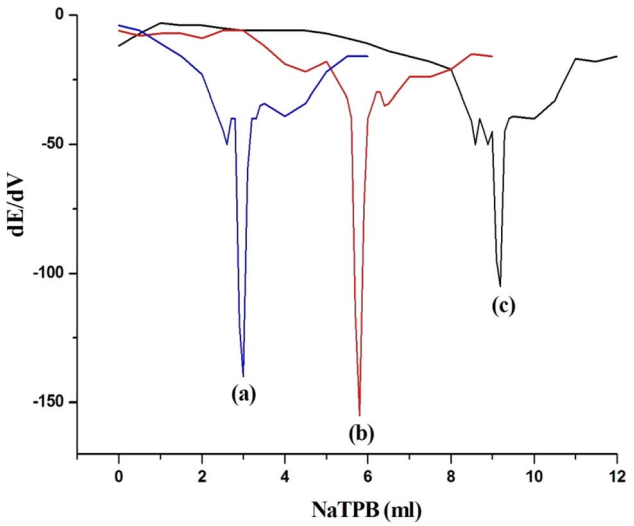

Fig. 8 First order derivative of potentiometric titration curves of (a) 3, (b) 6 and (c) 9 mL of 1.0×10^{-2} mol L^{-1} DTZ and 10^{-2} mol L^{-1} NaTPB as titrant using DTZ-CP sensor.

production of hazardous compounds have increased in response to the current state of global warming and the hazards it poses.[46] Green analytical chemistry (GAC) is a subfield of green chemistry that focuses on creating analytical techniques that are safe for people and the environment without affecting analytical figures of merit.[47] GAC principles are adaptable to a variety of analytical techniques, and the most recent studies demonstrate significant efforts in this area.[48] Electrochemistry is considered a straightforward method that enables fast sample measurement without the need for prior sample collection or pretreatment. To assess the greenness of analytical methods, several tools have been developed, including the Analytical Eco-scale, Green Analytical Procedure Index (GAPI), National Environmental Methods Index (NEMI), and Analytical GREEnness metric (AGREE). In this study, the Analytical Eco-scale and AGREE metric were applied to evaluate the proposed sensor.[47]

3.12 Analytical eco-scale

On the eco-scale, an excellent analytical technique would receive a score of 100 and Penalty points are deducted from the overall score for each deviation from this ideal in the parameters of the proposed method.

According to the results, a score of 75 or more indicates great green analysis, a score of 50 or higher indicates good green analysis, and a score of less than 50 indicates inadequate green analytical practice. Among the factors assessed are the type and amount of chemicals used, the energy consumption of different electric equipment, the amount of trash and how it is managed, and occupational dangers.[49] As shown in Table 5, our suggested approach is evaluated and proved to be an effective green analytical technique.

3.13 Analytical GREEnness metric (AGREE)

The method's greenness was evaluated using a comprehensive metric system that takes into account the 12 principles of green

Table 4 Comparison of the constructed DTZ-CP sensor method with published methods[a]

Method	Linear range (mol L^{-1})	Detection limit (mol L^{-1})	Response time (s)	Applications	Ref.
HPTLC	8.8×10^{-8}–8.8×10^{-7}	4.4×10^{-8}	—	Bulk drug and pharmaceuticals	7
Spectrophotometric	—	1.10×10^{-4}	—	Commercial tablets and capsules	10
Cyclic voltammetry	2.0×10^{-6}–8.0×10^{-5}	7.0×10^{-8}	—	Pharmaceutical formulation (capsule) and urine	11
	1.0×10^{-11}–15.0×10^{-8}	3.0×10^{-11}		Methyldopa	12
PVC membrane	1.0×10^{-5}–1.0×10^{-1}	7.09×10^{-6}	12	Pharmaceutical formulation and urine	13
DTZ-CPS	1.0×10^{-6}–1.0×10^{-2}	4.6×10^{-7}	10	Urine and industrial water	P.S.

[a] P.S.: present study.

Table 5 Details of the proposed technique's penalty points

Risk factors	Values	Hazardous (pictograms × hazard)	Penalty points
Reagents and solvents			
Graphite powder	<10 mL g^{-1}	2 × 1	2
O-NPOE	<10 mL g^{-1}	4 × 1	4
Instruments			
Energy	<0.1 kWh per sample	0	0
Waste	<10 mL	5	5
Heater	Non	0	0
Occupational hazards	Non	0	0
pH of the sample	2–12	0	0
Sample filtration	Non	0	0
Total penalty points	11		
AES score	100–11 = 89		

analytical chemistry. In the center of a segmented pictogram, the final score is displayed. Each criterion is given a color and a weight that reflect the effectiveness of the analytical process function. A greener process is indicated by a final score closer to 1, accompanied by a darker green coloration in the center and across each segment of the pictogram.[50] The suggested approach achieved a score of 0.81 and displayed a green center (Fig. 9), making it an environmentally friendly method of analysis.

3.14 RAPI and BAGI assessments

White Analytical Chemistry (WAC), introduced in 2021,[51] extends and complements green analytical chemistry by combining ecological, analytical, and practical perspectives according to the red–green–blue (RGB) model.[52]

As part of the present work, the Blue Applicability Grade Index (BAGI) and the Red Analytical Performance Index (RAPI), two recently introduced evaluative metrics, were employed to comprehensively assess the developed analytical methodology. BAGI, complementary to established green metrics, focuses on the practical relevance and real-world applicability of a method, allowing straightforward identification of its strengths and weaknesses and enabling objective comparison between different analytical approaches.[53] RAPI, provides a broader evaluation encompassing functional and validation-related aspects, including efficiency, sensitivity, and waste

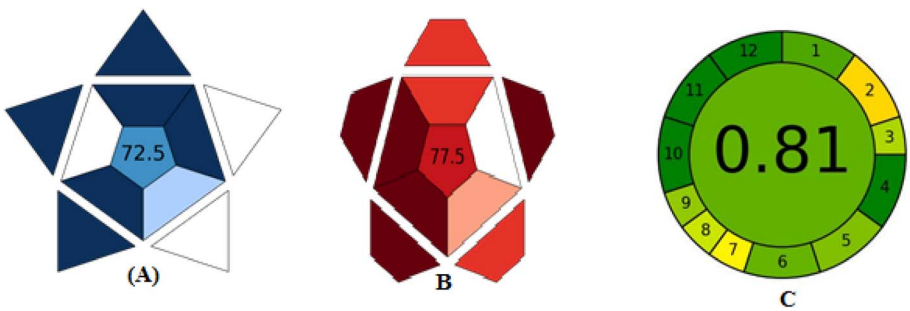

Fig. 9 Evaluation of the DTZ-CP sensor using: (A) BAGI for practical applicability, (B) RAPI for analytical performance, and (C) AGREE for environmental sustainability.

generation.[54] By integrating BAGI and RAPI with greenness metrics, a holistic assessment of an analytical method can be achieved, ensuring that environmentally friendly procedures are also robust, reliable, and suitable for practical applications. For each metric, a corresponding pictogram is automatically generated asteroid-shaped for BAGI and star-like for RAPI illustrating the evaluated criteria, with the final mean quantitative score (0.0–100.0) displayed at the center. Based on the comprehensive White Analytical Chemistry (WAC) evaluation, the developed DTZ sensor achieved RAPI and BAGI scores of 77.50 and 72.50 (Fig. 9), respectively, indicating its good performance, practicality and applicability within the proposed White Analytical Chemistry framework.

4. Conclusion

A novel and environmentally friendly potentiometric sensor composed of DB18C6 as a sensing ionophore for DTZ determination is constructed and described in the present study. The sensor's Nernstian slope of 57.4 ± 0.81 mVdecade^{-1}, rapid response time (10 s), long operational lifespan (6 weeks), and wide pH range of 2.0–8.0 demonstrated significant sensitivity and adequate selectivity towards DTZ. The sensor's potential stability and response time were enhanced by the modification with conducting polymer, which promoted electron transfer processes. The developed sensor can be applied to determine DTZ in pure drug samples, pharmaceutical formulations, human urine, and industrial water. In addition to experimental evaluation, the sensor was evaluated using AGREE, BAGI, and RAPI metrics to assess environmental greenness, sustainability, applicability, and overall analytical performance. The obtained pictogram scores (0–100 scale) confirmed the robustness, reliability, and practical suitability of the proposed sensor. Although DTZ was successfully detected, future studies will focus on enhancing sensitivity through alternative sensing strategies and measurement approaches.

Conflicts of interest

There are no conflicts to declare.

Data availability

The data that support the findings of this study are available from the corresponding author upon reasonable request.

References

1 S. Nazir and R. A. Iqbal, *Biosens. Bioelectron. X.*, 2023, **14**, 100388.
2 C. Lahoud, W. Hovater, A. Rosenberg, G. W. Makhoul, G. Vatandoust and M. Maruf, *Med. Rep.*, 2025, **10**, 100181.
3 I. E. Mozu, A. F. A. Marfo, J. S. Marfo, N. O. Adomako, N. K. Ayisi-Boateng, P. Boachie-Ansah, J. Attakorah and F. T. Owusu-Daaku, *ERCSP*, 2023, **12**, 100381.
4 Y. P. Timsina, P. Pandey, I. H. Mondal and A. H. Dark, *Food Chem. Adv.*, 2023, **3**, 100406.
5 A. Bathinapatla, S. Kanchi, R. Chokkareddy, R. P. Puthalapattu and M. R. Kumar, *Microchem. J.*, 2023, **192**, 108930.
6 A. B. Hall, K. Wilson, S. Guggino and F. Blind, *Am. J. Emerg. Med.*, 2024, **84**, 15–17.
7 P. V. Devarajan and V. V. Dhavse, *J. Chromatogr. B Biomed. Appl.*, 1998, **706**, 362–366.
8 N. Li, C. Li, N. Lu and Y. Dong, *J. Chromatogr. B*, 2014, **967**, 90–97.
9 T. Alebić-Kolbah and F. Plavšić, *J. Pharm. Biomed. Anal.*, 1990, **8**, 915–918.
10 N. Rahman and S. N. H. Azmi, *Microchem. J.*, 2000, **65**, 39–43.
11 M. Ghandour, E. Aboul Kasim, A. M. Ali, M. El-Haty and M. M. Ahmed, *J. Pharm. Biomed. Anal.*, 2001, **25**, 443–451.
12 R. Imani, M. Shabani-Nooshabadi and N. Ziaie, *Chemosphere*, 2022, **297**, 134170.
13 M. R. Ganjali, T. Razavi, R. Dinarvand, S. Riahi and P. Norouz, *Int. J. Electrochem. Sci.*, 2008, **3**, 1543–1558.
14 M. H. Sorouraddin, M. Saadati and F. Mirabi, *J. Food Drug Anal.*, 2015, **23**, 1543–1558.
15 A. Yarahmadi, T. Madrakian, A. Afkhami and N. R. Jalal, *J. Electrochem. Soc.*, 2019, **166**, B1268–B1275.
16 Ir. S. Muratova, L. A. Kartsova and K. N. Mikhelson, *Sens. Actuators, B Chem.*, 2015, **207**, 900–906.
17 M. Elhassan, A. M. Mahmoud, M. A. Hegazy, S. Mowaka and J. G. Bell, *Talanta*, 2025, **287**, 127623.
18 O. Özbek and O. C. Altunoluk, *Sens. Int.*, 2023, **4**, 100224.
19 M. A. Korany and R. K. Mahmoud, *Microchemical. J.*, 2021, **171**, 106890.
20 A. Lochab, S. Baxi, P. Tiwari, S. Bardiya and R. Saxena, *Microchem. J.*, 2024, **199**, 109923.
21 I. Khan, K. Saeed and I. Khan, *Arab. J. Chem.*, 2019, **12**, 908–931.
22 M. Rabia, E. Aldosari, A. M. Elsayed, A. sanna and O. Farid, *Opt. Quant. Electron.*, 2024, **56**, 1–17.
23 E. Aldosari, M. Rabia and A. A. A. Abdelazeez, *Green Process Synth.*, 2023, **13**, 20230243.
24 N. Ermiş and N. Tinkilic, *Electroanalysis*, 2021, **33**, 20230243.
25 S. S. Soliman, A. M. Mahmoud, M. R. Elghobashy, H. E. Zaazaa and G. A. Sedik, *Talanta*, 2024, **267**, 125238.
26 F. Alkallas, A. M. ELsayed, A. B. G. Trabelsi and M. Rabia, *Phys. Scr.*, 2024, **99**, 65972.
27 A. M. ELsayed, M. A. Alnuwaiser and M. Rabia, *J. Mater. Sci.: Mater. Electron.*, 2023, **34**, 65972.
28 E. M. S. Azzam, H. M. Abd El-Salam and R. S. Aboad, *Polym. Bull.*, 2019, **76**, 1929–1947.
29 M. Rabia, A. B. G. Trabelsi, F. H. Alkallas and A. M. ELsayed, *Phys. Scr.*, 2024, **99**, 65972.
30 F. A. Christy and P. S. Shrivastav, *Crit. Rev. Anal. Chem.*, 2011, **41**, 236–269.
31 K. N. Mikhelson and M. A. Peshkova, *Russ. Chem. Rev.*, 2015, **84**, 555–578.
32 S. O. Mirabootalebi and Y. Liu, *Analyst*, 2024, **149**, 3694–3710.
33 M. A. Korany, S. A. Abdel Moaty and M. M. Khalil, *Sens. Actuators, B Chem.*, 2018, **273**, 429–438.

34 A. Konefal, P. Piatek, B. Paterczyk, K. Maksymiuk and A. Michalska, *Talanta*, 2023, **2539**, 124038.
35 D. A. Armbruster and T. Pry, *Clin Biochem Rev.*, 2008, (Suppl 1), S49–S52.
36 H. S. Magar, R. Y. A. Hassan and A. Mulchandani, *Sensors*, 2021, **21**, 6578.
37 S. M. Mostafa, A. A. Farghali and M. M. Khalil, *Electroanalysis*, 2021, **33**, 1194–1204.
38 M. Fibbioli, W. E. Morf, M. Badertscher, N. F. de Rooij and E. Pretsch, *Electroanalysis*, 2000, **12**, 1286–1292.
39 E. Elgazzar, K. Attala, S. Abdel-Atty and A. M. Abdel-Raoof, *Talanta*, 2022, **242**, 123321.
40 R. P. Buck and E. Lindner, *Pure Appl. Chem.*, 1994, **66**, 2527–2536.
41 Y. Umezawa, K. Umezawa and H. Sato, *Pure Appl. Chem.*, 1995, **67**, 507–518.
42 M. Shamsipur, A. A. M. Beigi, M. Teymouri, S. Rasoolipour and Z. Asfari, *Anal. Chem.*, 2009, **81**, 6789–6796.
43 E. Bakker and E. Pretsch, *Anal. Chem.*, 2002, **74**, 420–426.
44 C. M. Choi, J. Heo and N. J. Kim, *Chem. Cent. J.*, 2012, **6**, 84.
45 C. J. Pedersen, *J. Am. Chem. Soc.*, 1967, **89**, 7017–7036.
46 S. H. Abdelaal, N. F. El Azab, S. A. Hassan and A. M. El-Kosasy, *Acta Part A Mol. Biomol. Spectrosc.*, 2021, **261**, 120032.
47 M. Sajid and J. Płotka-Wasylka, *Talanta*, 2022, **238**, 123046.
48 M. Gamal, I. A. Naguib, D. S. Panda and F. F. Abdallah, *Anal. Methods*, 2021, **13**, 369–380.
49 S. A. Atty, H. R. A. El-Hadi, B. M. Eltanany, H. E. Zaazaa and M. S. Eissa, *Electrocatalysis*, 2022, **13**, 731–746.
50 F. Pena-Pereira, W. Wojnowski and M. Tobiszewski, *Anal. Chem.*, 2020, **92**, 10076–10082.
51 P. M. Nowak, R. Wietecha-Posłuszny and J. Pawliszyn, *TrAC, Trends Anal. Chem.*, 2021, **138**, 116223.
52 P. M. Nowak and P. Kościelniak, *Anal. Chem.*, 2019, **91**, 10343–10352.
53 N. Manousi, W. Wojnowski, J. Płotka-Wasylka and V. Samanidou, *Green Chem.*, 2023, **25**, 7598.
54 P. M. Nowak, W. Wojnowski, N. Manousi, V. Samanidou and J. Płotka-Wasylka, *Green Chem.*, 2025, **27**, 5546.